JOURNAL OF OPTOELECTRONICS AND ADVANCED MATERIALS Vol. 10, No. 10, October 2008, p. 2603 - 2606

The optical and structural properties of ZnO:Mn nano films grown by sol-gel

M. YUONESI[a, b*], M. E. GHAZI[a], M. IZADIFARD[a], M. YAGHOBI[a]
[a]*Physics Department, Shahrood University of Technology, Shahrood-Iran*
[b]*Department of Physics, Islamic Azad University-Ayatolla Amoli Branch, Amol, Iran*

There are many techniques used to deposit high-quality ZnO thin films. One of these based on chemical method for the production of ZnO thin films is the sol-gel. ZnO:Mn nano films doped with manganese different concentrations were deposited on glass substrates by the spin-coating method. The precursors for the synthesis ZnO:Mn are: Zinc acetate dehydrate, manganese acetate dehydrate, 2-mithoxyethanol and monoethanolamine as zinc and manganese source, solvent and stabilizer respectively. Seven samples of diluted magnetic semiconductors ZnO:Mn were prepared with different atomic ratio Mn/Zn. Characterization techniques of XRD, EDX and UV-visible spectra measurements were done to investigate the effects of Mn doping concentration on the optical and structural properties of ZnO:Mn nano films. The XRD patterns of all nano films show the crystallization behavior and are hexagonal wurtzite structure for different x, without existing other phases. Our results reveal that with high percent manganese not only the degree of crystalline decreases but also peak broadening occurs. The compositional analysis was carried out by energy dispersive X-ray (EDX) measurement. Compositional analysis shows 0.00, 0.01, 0.018, 0.029, 0.041, 0.05 and 0.059 Mn/Zn ratios in samples. The optical studies show that the band gap of ZnO:Mn decreases for smaller x than 0.03 from 3.3 to 3.26 because there are a strong interaction between localized moments of the d electrons of Mn atom and band carriers of host material, and increases for higher x than 0.03 because of the structural changes of the material.

(Received May 5, 2008; accepted August 14, 2008)

Keywords: Zinc oxide, Sol-gel, Semiconductors, Spintronics, DMS

1. Introduction

Diluted magnetic semiconductors (DMS) for spintronics with Curie temperature above room temperature are receiving increasing attention in recently two decades. Spintronics, or spin electronics, refers to the study of the role played by electron (and nuclear even) spin in solid state physics, and possible devices that specifically exploit spin properties instead of or in addition to the charge degrees of freedom. There are many theoretical and experimental studies in this area for different materials. The theoretical predictions which was carried out by Dietl [1] show many DMS being ferromagnetism at room temperature and are suitable for applying in spintronics. One of these materials is ZnO which is a II-VI semiconductor compound and has a direct band gap around 3.2-3.37 eV in 300 K [2,3] with high exciton binding energy of 60 mev and is a wide direct band gap semiconductor. Zinc oxide is normally formed in hexagonal (wurtzite) crystal structure with a=3.25 Å and c=5.12 Å and has 6-mm symmetry. Four O atoms tetrahedrally coordin-ate with one Zn atom in semiconductor and the p- orbital electrons of the O atom hybridize the d-orbital electrons of the Zn atom. The pure ZnO thin films are naturally n-type semiconductor which has the electric-al conductivity due to either oxygen vacancy or interstitial Zn that there are in ZnO lattice sites. Energy levels of the intrinsic defects are approxima-tely 0.05 eV down the conduction band. The physical properties of ZnO films strongly depend on the deposition methods. As a example, we can name resistivity of ZnO film that alters from 10^{-4} to 10^{10} $\Omega.cm$. In the room temperature for ZnO single crystal, hall mobility is approximately 200 $cm^2/V.s$. Due to unique properties of ZnO films such as low electric resistance, high transparency in the visible light, piezoelectricity, high voltage-current nonlinearity and chemical stability [4], there are different applications. as example, we can name it applications in bulk acoustic and surface acoustic wave solar cells, transparent electrodes, blue UV light emitter device and gas sensor [5-10].There are many techniq-ues used to deposit high-quality ZnO thin films and nano films, such as r.f or dc sputtering, pulsed laser deposition (PLD), ionplating, chemical vapor deposi-tion (CVD), thermal evaporation, spray pyrolysis and molecular beam epitaxy (MBE)[11-16]. One of another method based on chemical method for the production of ZnO thin films is sol-gel which is widely used in the synthesis of ZnO nano crystals. The sol-gel process [17] is simple, inexpensive in fabrication, to produce a large number of samples, easier composition control and the accurately controlled mole ratio, the high solubility, better homogeneity, lower processing temperature and has a general advantage for large area deposition and thickness of the films.

2. Experimental method

ZnO:Mn nano films are prepared by the sol-gel. In this experimental work, three steps utilized are preparation of materials, synthesis and characterization techniq-ues. In continuing, we will explain any section.

2.1. Preparation of materials

The precursors utilized for the synthsis ZnO:Mn are: Zinc acetate dehydrate $[Zn(CH_3Coo)_2 - 2H_2o]$, manganese acetate dehydrate $[Mn(CH_3Coo)_2 - 2H_2o]$, 2-mith oxyethanol (DME) $[C_3H_8O_2]$ and monoethanolamine (MEA) $[C_2H_7NO]$ as zinc and manganese source, solvent and stabilizer respectively. All chemical materials were prepared from Merck Company, and were applied without more purification.

2.2. Synthesis

All seven samples of ZnO:Mn nanofilms were prepared by the sol-gel method. First, at room temperature, zinc acetate and dopant were dissolved in a mixture of DME and MEA solution. The molar ratio of MEA to Zn^{+2} was maintained at 1. Solutions were prepared with containing zinc acetate, manganes acetate from 0 to 6%, DME and MEA. At 70 ^oC, solutions were vigorously stirred for 1 h by means of a magnetic stirrer to yield a clear and homogeneous solution. At room temperature, the coating solutions were aged for at least one day, and then deposited on glass slid substrates, which were cleaned prior, by spin coating. Undoped ZnO precursor was prepared in the same way.

The solution were dropped onto the glass slid substrates which were rotated at 3000 rpm for 30 s. after depositing by spin coating, the films were dried at 250 ^oC for 10 min to evaporate the solvent and remove organic residuals. This procedure, from depositing to drying, was repeated six times for reaching to the desired thickness. In an open air furnace, the films were finally heated at 450 ^oC for 1h. Samples for characterizations become slightly cold until the room temperature.

2.3. Characterization techniques

In this work, our intent is the investigation of band gap in ZnO:Mn nano films then avoided other further characterizations. The desirable characterizations are X-ray diffraction, compositional analysis and UV/Vis spectra measurements for investigating the effects of doping concentration on the properties of Zno:Mn nano films.

3. Results and discussion

3.1. Chemical composition

For determining composites in different doping Mn concentration of ZnO:Mn nano films, compositional analysis was performed on Philipps XL 20 by energy dispersive X-ray (EDX) analysis. for investigating the effects of dopant concentration on the bang gap properties of ZnO:Mn nano films, seven types of samples were prepared with seven Mn/Zn atomic ratio 0-6%., But the EDX analysis finally showed other different values with comparing the dopant Mn concentration in the starting precursors. There are compositional analyses of all samples in Table 1.

Table 1. Compositional analyses of seven samples

sample	1	2	3	4	5	6	7
Mn/Zn at %	0.0	1.0	1.8	2.9	4.1	5.0	5.9

Fig. 1 shows spectra measurements for the 6th sample.

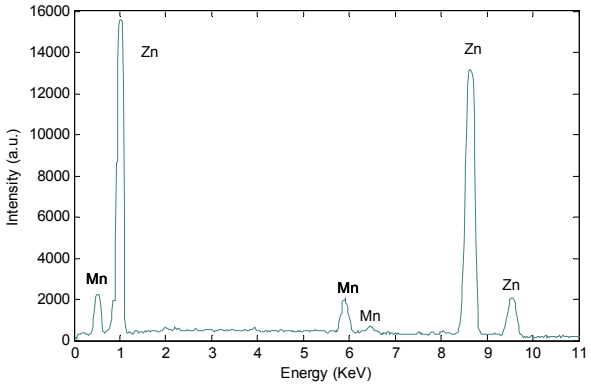

Fig.1. EDX spectra of 5.0% Mn doped concentration.

3.2. XRD studies

The x-ray diffractometer (XRD 6000, Shimadzu, Japan) with CuK_α line radiation (λ = 1.5406 Å) was used for crystallite phase and determining orientation. Fig. 2 shows XRD-ray patterns of all samples which were deposited on the glass substrates. The diffraction patterns reveal a good crystalline without any appreciable changes from pure ZnO films and are genuine polycrystalline with the hexagonal wurtzite structure. These results imply that there are no secondary phases such as manganese cluster or oxides. our results reveal that with increasing percent manganese not only the quality of crystalline decreas-es but also peak broadening occurs (particularly for small peak), that it may be due to ionic radius of Mn^{2+} (0.83 Å) that is larger than ionic radius of Zn^{2+} (0.74 Å). This phenomenon in the films creates a strain or stress because of mismatching Mn^{2+} in the Zn^{+2} lattice site. However, the crystal quality of films decreases with increase of Mn percentage [18].

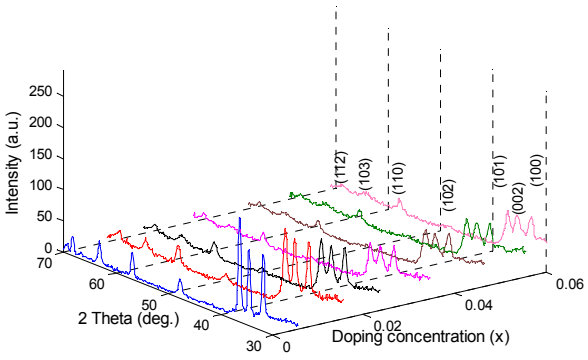

Fig. 2 XRD patterns of ZnO nano films as a function of Mn doping concentration.

3.3. Uv-Vis analysis

Room temperature optical transmittance was measured by a UV-Vis spectrophotometer (Varian Cary100). Fig. 3 shows the optical transmittance spectra of the films in the wavelength region range from 350 to 800 nm.

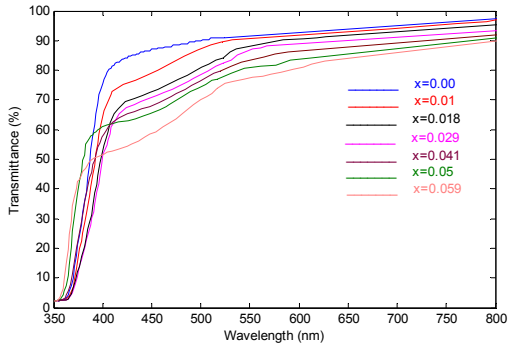

Fig. 3. Dependence of optical transmission on wavelength for ZnO nano films of various values of Mn doping concentration.

It is evident that the optical transmittance increases in the visible region, and decreases in the UV region for a sample. With the increase of 0-6% manganese concentration, the optical transmittance spectra of the samples gradually decrease in the Vis region. Transmittance in undoped film is almost 90-95% for Vis region.

The optical band gap of the Mn-doped ZnO nano films was estimated by extrapolation of the linear relationship $(\alpha h\nu)^2 = h\nu - E_g$, where α is the absorption coefficient, $h\nu$ is the photon energy, E_g is the optical band gap of nano films. It is determined by theory of the direct optical absorption. Fig. 4 shows the $(\alpha h\nu)^2$ vs. photon energy curves of ZnO nano films with varying doping concentration.

Fig. 5 shows the band gap of all samples vs. manganese concentration. It is evident from figure that the band gap initially decreases with increase of manganese blow 3% and there is initially a red shift but with the increase of manganese above 3%, a blue shift occurs.

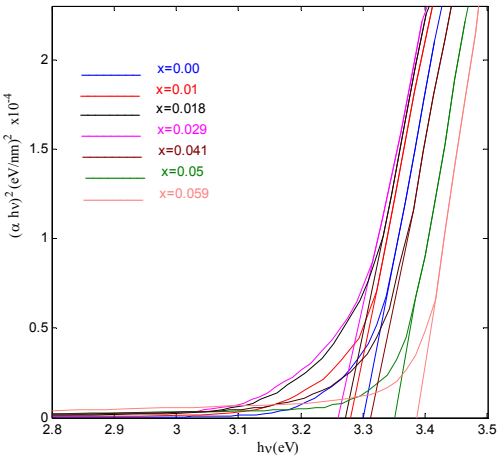

Fig. 4 The plot of $(\alpha h\nu)^2$ vs $h\nu$ for ZnO nano film with different values of Mn doping concentration.

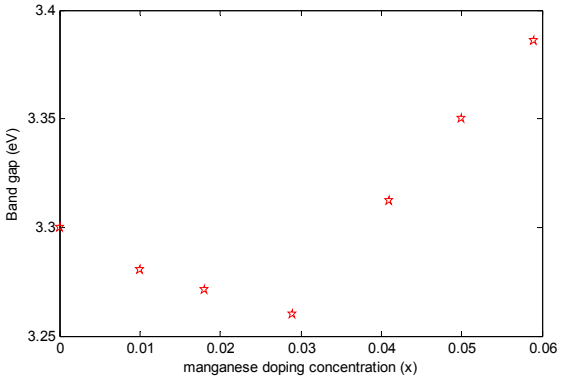

Fig. 5. Dependence of The optical band gap of the Mn-doped ZnO nano films as a function of Mn doping concentration.

One of II-VI DMS which have a paramagnetic phase is ZnO. Many features of DMS, such as the special electronic properties, unique phase diagrams, and important magnetic and magneto-optical characteristi- cs, are induced by the exchange interaction between the localized *d* shell electrons of the magnetic ions and the delocalized band states (of s or p origin). The presence of magnetic impurity creates two potentials in ZnO thin film. One part is related to the difference of the potential between the changes of atomic variety of Mn^{+2} in Zn^{+2} lattice sites, and another is magnetic potential of Mn^{+2} ions. We neglect first potential due to be small and consider second potential. Suppose the state of Mn ions in DMS material is Mn^{+2}. The electronic structure of Mn^{+2} is $1s^2\ 2s^2\ 2p^6\ 3s^2\ 3p^6\ 3d^5$, in which *3d* is a half-filled shell. According to Hund's rule, the spin of these five 3d electrons will be parallel to each other, so the total spin is $S = 5/2$. These five electrons are in states in which the orbital angular momentum quantum number $l = 0,\pm1,\pm2$. Thus the total orbital angular momentum is $L = 0$. The

total angular momentum for a Mn^{+2} ion then is $J = S = 5/2$. The Land´e g-factor is

$$g = 1 + \frac{J(J+1) + S(S+1) - L(L+1)}{2J(J+1)} = 2 \qquad (1)$$

In the non-interacting paramagnetic phase without a external magnetic field, the magnetic momentum for Mn^{+2} is $\mu_I = (-ge/2cm_0)\mathbf{I}$ where $I_s = 5/2,\ 3/2,\ 1/2,\ -5/2,\ -3/2,\ -1/2$, and the exchange Hamiltonian of one band electron with spin S interacting with the $3d^5$ electrons from a Mn^{+2} ions is

$$H_{ex} = -\frac{8\pi}{3}\boldsymbol{\mu}_e \cdot \boldsymbol{\mu}_I \delta(\mathbf{x}) + \frac{1}{r^3}\left[\boldsymbol{\mu}_e \cdot \boldsymbol{\mu}_I - 3\frac{(\mathbf{x}\cdot\boldsymbol{\mu}_e)(\mathbf{x}\cdot\boldsymbol{\mu}_I)}{r^2}\right] \qquad (2)$$

The expectation values of this Hamiltonian in the various atomic states yield the energy shifts. For spherically symmetric s states the second term gives a zero expectation value. The energy comes from the first term:

$$E_{ex}^{c} = \langle \psi_{ck}(\mathbf{r}) | H_{ex} | \psi_{ck}(\mathbf{r}) \rangle = -\frac{8\pi}{3}|\psi_{ck}(0)|^2 \langle \boldsymbol{\mu}_e \cdot \boldsymbol{\mu}_I \rangle = -\frac{8\pi}{3}|\psi_{ck}(0)|^2 \left(\frac{\hbar e}{c}\right)^2 \left(\frac{1}{m_I m_e}\right)\left(\frac{S\cdot I}{\hbar^2}\right) \qquad (3)$$

And

$$\left(\frac{S\cdot I}{\hbar^2}\right) = \frac{1}{2}\left[F(F+1) - S(S+1) - I(I+1)\right] \qquad (4)$$

$\mathbf{F} = \mathbf{S} + \mathbf{I}$ is the total spin. For $S = 1/2$ and $I = 5/2$, the total spin are 3 (seven states) and 2 (five states). For F=3, this is 5/4 and for F=2, it equals -7/4. These relations are valid for holes in valance band, and band gap changes to $E_g^0 - \left(E_{ex}^c + |E_{ex}^v|\right)$. Our experimental results show when dopant concentration is below 3%, F=3 is acceptable and the band gap $Zn_{1-x}Mn_xO$ decreases. Such an initial red shift in the band gap ZnO:Mn has been reported in the nineteenth reference [19].

The band gap in bulk for MnO and ZnO are 4.2 and 3.32eV respectively as seen, the band gap MnO is higher than ZnO. In this work, the band gap Zn_{1-x} Mn_xO increases for x above 3% as it expects.

4. Conclusions

Mn-doped ZnO nano films were prepared with different values of Mn content by a sol gel spin-coating method. X-ray diffraction, as one of the most useful and convenient tool, is done for the structural characterization. The diffraction patterns reveal a good crystalline with the hexagonal wurtzite structure. The elemental composition of the samples can be determined by energy disperse spectroscopy (EDX). EDX of samples were prepared with different values of Mn/Zn atomic ratio from 0 to 6%. Room temperature optical transmittance spectra of samples were performed and show that the visible transmission of films generally decreases with the increase of Mn content and is high (>90%). Due to the exchange interaction between the localized *d* shell electrons of the magnetic ions and the delocalized band states, the optical band gap E_g decreases from 3.3 to 3.26 eV for low doping concentration (x<3%) and, increases for high concentration(x>3%) due to the structural change of material from ZnO to MnO. This unique property of ZnMnO films can be used to band gap engineering for the production of quantum wells and super lattices and also have many applications in spintronics.

Reference

[1] T. Dietl, H. Ohno, F. Matsukura, J. Cibert, D. Ferrand. Science, **287**, 1019 (2000).
[2] D. P. Norton, M. Ivill, Y. Li, Y. W. Kwon, J.M. Erie, H. S. Kim, K. Ip, S. J. pearton, Y. W. Heo, S. Kim, B. S. Kang, F. Ren, A. F. Hebard, J. Kelly, Thin Solid Films **496,** 160 (2006).
[3] A. Jain, P. Sagar, R. M. Mehra, Materials Science Poland **25**, 1 (2007).
[4] D. C. Look, Mater. Sci. Eng. B **80,** 383 (2001).
[5] C. Lee, K. Lim, J. Song, Sol. Energy Mater. Sol. Cells **43,** 37 (1996).
[6] T. Negami, Y. Hashimoto, S. Nishiwaki, Sol. Energy Mater. Sol. Cells **67**, 331 (2001).
[7] Y. Natsume, Thin Solid Films **372**, 30 (2000).
[8] G.K. Paul, S. Bandyapadhyay, S. K. Sen, Phys. Stat. Sol. A 191.
[9] D.C. Look, D.C. Reynolds, C.W. Litton, R.L. Jones, D.B. Eason
[10] X. Wang, W. P. Careg, S. Yee, Sensors Actuators B **28**, 63 (1995).
[11] H. Soto, T. Minami, T.Miyata, S. Takata, M. Ishii, Thin Solid Films **246**, 65 (1994).
[12] D. H. Zhang, D. E. Brodie, Thin solid Films **238**, 95 (1994).
[13] M. Jin, L.S. Ying, thin solid films **237**, 16 (1994).
[14] Y. Ly, G.W. Meng, L.D. Zhang, Appl. Phys. Lett. **76**, 2011 (2000).
[15] Y.C. Wang, I.C. Leu, M.H. Hon, J. Cryst. Growth **237**, 564 (2002).
[16] S.S. Lin, J.L. Huang, D.F. Lii, Surf. Coat. Technol. **176,** 173 (2004).
[17] P. Sagar, M. Kumar, R.M. Mehra, Thin Solid Films, **486**, 94 (2005)
[18] J.H Lee, B.O Park. Thin Solid Films **426,** 94 (2003).
[19] Hua-Wei Zhang, Er-Wei Shi, Zhi- Zhan Chen, Xue-Chao Liu, Bing Xiao, Li-Xin Song, Journal of Magnetism and Magnetic Materials **305,** 377 (2006).

*Corresponding author: myuonesi@gmail.com